Biophysical Journal Volume 66 May 1994 1642–1652

Carbohydrate Dynamics at a Micellar Surface: GD1a Headgroup Transformations Revealed by NMR Spectroscopy

Leszek Poppe,* Herman van Halbeek,* Domenico Acquotti,‡ and Sandro Sonnino‡

*Complex Carbohydrate Research Center and Department of Biochemistry, The University of Georgia, Athens, Georgia 30602 USA, and ‡Center for Functional Biochemistry of Brain Lipids, Department of Medicinal Chemistry and Biochemistry, The Medical School, University of Milan, 20133 Milan, Italy

ABSTRACT The conformational dynamics of the carbohydrate headgroup of ganglioside GD1a, NeuAcα2→3Galβ1→3GalNAcβ1→4[NeuAcα2→3]Galβ1→4Glcβ1→1Cer, anchored in a perdeuterated dodecylphosphocholine micelle in aqueous solution, were probed by high resolution NMR spectroscopy. The observed $^1H/^1H$ NOE interactions revealed conformational averaging of the terminal NeuAcα2→3Gal and Galβ1→3GalNAc glycosidic linkages. The pronounced flexibility of this trisaccharide moiety was substantiated further by two-dimensional proton-detected ^{13}C T_1, $T_{1\rho}$ and $^1H/^{13}C$ NOE measurements. The anchoring effect of the micelle allowed the detection of conformational fluctuations of the headgroup on the time scale of a few hundred picoseconds. NMR experiments performed on the GD1a/DPC micelles in H_2O at low temperatures permitted the observation of hydroxyl proton resonances, contributing valuable conformational information.

INTRODUCTION

Cell surface glycolipids are involved in a variety of specific interactions such as cell-cell adhesion, cell differentiation, malignant transformations, and signal transduction (Hakomori, 1984; Fishman and Brady, 1976; Hakomori, 1993). It is believed that the conformations and dynamics of the oligosaccharide moiety play key roles in the biological functions of glycolipids. The structures of glycolipids at the molecular level have been studied by NMR spectroscopy in both liquid and liquid-crystalline solutions. The NMR methodology, however, differs considerably between the two types of media. In oriented, membrane-like systems, orientation and dynamics of the glycolipid headgroup have been probed by dipolar, ^{13}C-^{13}C, ^1H-^{13}C (Sanders II and Prestegard, 1991; Aubin and Prestegard, 1993), or deuterium quadrupolar (Skarjune and Oldfield, 1979; Jarrell et al., 1986; Fenske et al., 1991; Winsborrow et al., 1991) couplings. Although potentially very powerful, these studies require isotopic enrichment, which is not currently a routine procedure. Alternatively, suitable systems for high resolution NMR studies are native glycolipids dissolved in aprotic solvents (Czarniecki and Thornton, 1977; Scarsdale et al., 1986; Scarsdale et al., 1990; Acquotti et al., 1990; Poppe et al., 1990), the oligosaccharide portions of the glycolipid molecules dissolved in water (Sabesan et al., 1984; Sabesan et al., 1991) and glycolipid/detergent aqueous solutions (London and Avitabile, 1976; Eaton and Hakomori, 1988; Poppe et al., 1990; Acquotti et al., 1990). The latter system is particularly attractive because the glycolipid is anchored in a detergent micelle that, to a certain extent, resembles the physiological membrane environment, yet is small enough to give high-resolution spectra.

The ganglioside GD1a is a dianionic glycolipid (Scheme 1) that is found predominantly in neuronal plasma membranes. To date, the conformation of the hexasaccharide portion of GD1a has been probed at the levels of both the native ganglioside dissolved in DMSO solution (Scarsdale et al., 1990) and a lipid-free, synthetic oligosaccharide analog, GD1aOS, in aqueous solution (Sabesan et al., 1991). These independent studies revealed rather rigid, yet different conformations for the headgroup. This discrepancy, most likely due to different solvent effects on the carbohydrate conformation, prompted us to probe the three-dimensional structure of GD1a in a more natural environment, such as a phospholipid (DPC) micelle in aqueous solution. This system facilitated the use of high resolution NMR experiments that comprised single-selective and double-selective ^1H NOE measurements, involving labile and nonlabile protons. In addition, the molecular dynamics of the ganglioside headgroup were studied by probing $^{13}C/^1H$ dipolar interactions through ^{13}C T_1, $T_{1\rho}$, and NOE measurements.

MATERIALS AND METHODS

Sample preparation

Ganglioside GD1a was isolated from calf brain as previously described (Tettamanti et al., 1973). Samples for NMR measurements were prepared by dissolving 7 mg of the sodium salt of the ganglioside and 77 mg of dodecylphosphocholine-d_{38} (DPC), purchased from Merck, Sharp and

Received for publication 6 December 1993 and in final form 4 February 1994.

Address reprint requests to Dr. Leszek Poppe, Complex Carbohydrate Research Center, The University of Georgia, 220 Riverbend Road, Athens, GA 30602-4712. Tel.: 706-542-4414; Fax: 706-542-4412.

Abbreviations used: 1D, one-dimensional; 2D, two-dimensional; Cer, ceramide; DANTE, delays alternated by nutation for tailored excitation; DEPT, distortionless enhancement by polarization transfer; DPC, dodecylphosphocholine-d_{38}; GalNAc, *N*-acetylgalactosamine; HMBC, heteronuclear multiple-bond correlation spectroscopy; HSQC, heteronuclear single-quantum coherence spectroscopy; INEPT, insensitive nuclei enhanced by polarization transfer; MINSY, mixing irradiation during NOESY; NeuAc, *N*-acetylneuraminic acid; NOE, nuclear Overhauser effect; NOESY, NOE correlated spectroscopy; ROESY, rotating-frame NOE correlated spectroscopy; TOCSY, total correlation spectroscopy; TPPI, time-proportional phase incrementation.

0006-3495/94/05/1642/11 $2.00

SCHEME 1

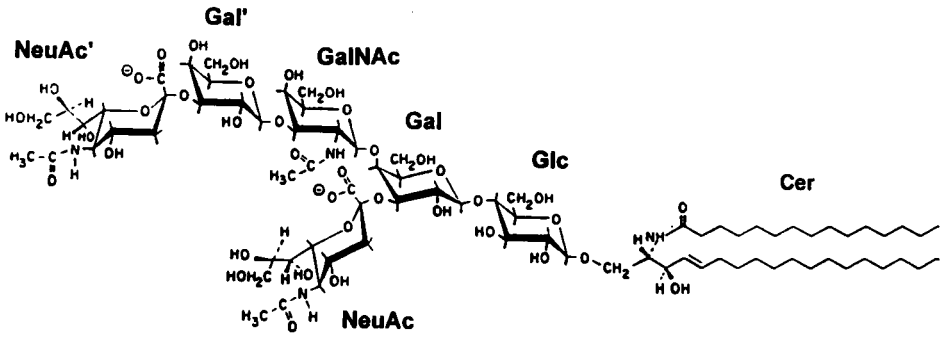

GD1a

Dohme (St. Louis, MO), in 0.5 ml of D_2O or 90% H_2O/10% D_2O. The D_2O solution contained phosphate buffer (pH 7) and was deoxygenated by bubbling with argon gas. To obtain the conditions of slowest chemical exchange for the hydroxyl protons, the pH of the H_2O solution was carefully adjusted with the addition of hydrochloric acid or sodium hydroxide to ~7.4.

NMR spectroscopy

Proton-detected spectra were obtained at 600 MHz using a Bruker AMX 600 spectrometer. The 1D NOESY (Neuhaus and Williamson, 1989), 1D MINSY (Massefski, Jr. and Redfield, 1988), 1D ROESY (Bothner-By et al., 1984), 1D TOCSY (Subramanian and Bax, 1987), and 1D double-selective TOCSY-NOESY (Boudot et al., 1990; Poppe and van Halbeek, 1992) spectra were recorded at 305 K using the selective, 90_x–$180_{x,\,y,-x,-y}$, excitation (Sklenár and Feigon, 1990) based on DANTE pulse trains (Morris and Freeman, 1978). Truncated NOE spectra (200–500 ms preirradiation time) in H_2O solution were obtained by using the 1-$\bar{1}$ echo water suppression technique (Sklenár and Bax, 1987; Poppe and van Halbeek, 1991). The 1D spectra were recorded with an acquisition time and relaxation delay of 1.1 and 1.5 s, respectively. Typically, 80–320 scans were accumulated per spectrum.

The 2D heteronuclear, ^1H-detected experiments were carried out at 305 K using TPPI for quadrature detection in the F1 dimension (Marion and Wüthrich, 1983). The 2D HSQC (32 scans per t_1 increment) and HSQC-NOESY (96 scans per t_1 increment, 0.25 s mixing time) spectra were recorded with t_2 and t_1 acquisition times of 340 and 28.2 ms, respectively, and a relaxation delay of 1.1 s. Pulse trains for ^{13}C relaxation and heteronuclear NOE measurements were based on the INEPT (for the CH) or DEPT-45° (for the CH_2) magnetization transfer steps (Sklenár et al., 1987; Kay et al., 1987; Kay et al., 1989; Nirmala and Wagner, 1989; Palmer III et al., 1991; Peng et al., 1991; Peng and Wagner, 1992). Fig. 1 shows examples of the

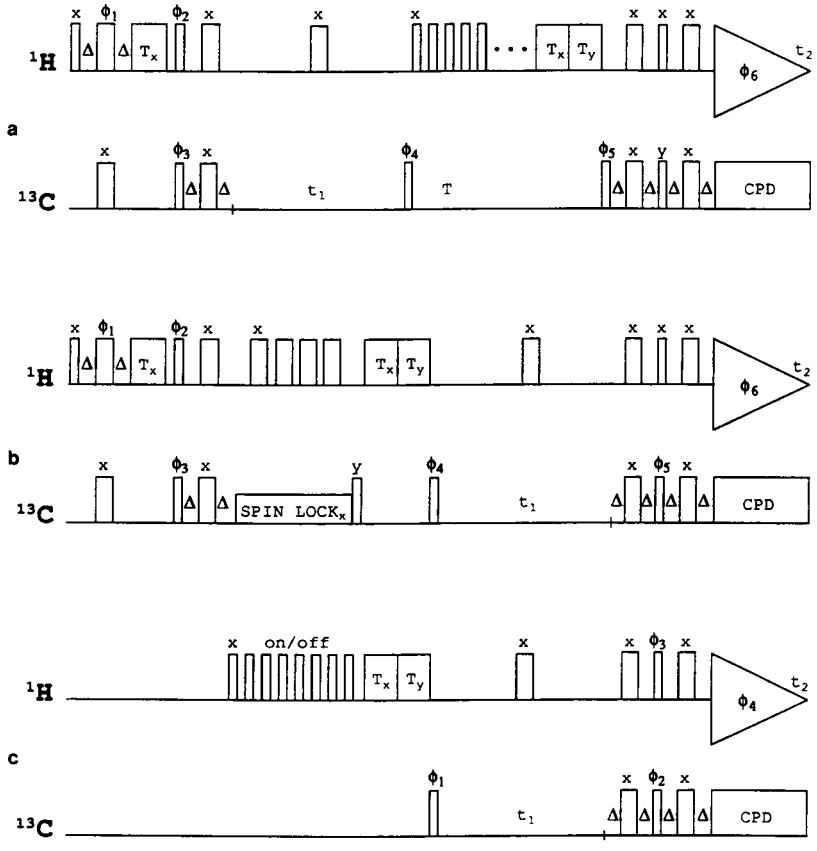

FIGURE 1 Pulse sequences for proton-detected T_1 (*a*), $T_{1\rho}$ (*b*), and NOE (*c*) measurements. The thin and thick bars denote 90 and 180° pulses, respectively. T_x, T_y stand for short trim pulses (1–2 ms), Δ = 1.5 ms. (*a*) $\phi_1 = 16x, 16y$; $\phi_2 = 8y, 8(-y)$; $\phi_3 = 4x, 4(-x)$, $\phi_4 = y, -y$; $\phi_5 = 2x, 2(-x)$; $\phi_6 = F^5(x, -x)$, where F denotes the fractal symmetry operation, i.e., $F(x, -x) = (x, -x, -x, x)$. (*b*) $\phi_1 = 8x, 8y$; $\phi_2 = 4y, 4(-y)$; $\phi_3 = 2x, 2(-x)$; $\phi_4 = 16(-y), 16y$, $\phi_5 = x, -x$; $\phi_6 = F^5(x, -x)$. The spin-lock consisted of contiguous carbon 180° pulses, interspersed with proton 180° pulses, to eliminate the effects from cross correlation between chemical-shift anisotropy and dipolar relaxation mechanisms (Peng and Wagner, 1992; Kay et al., 1992). (*c*) $\phi_1 = 2x, 2(-x)$; $\phi_2 = y, -y$; $\phi_3 = 4x, 4(-x)$; $\phi_4 = F^2(x, -x)$.

pulse schemes for measuring T_1, $T_{1\rho}$, and NOE (for the methine carbons). The T_1 and $T_{1\rho}$ spectra were recorded with mixing times of 40, 140, 220, 320, 500, 800, 1000, and 1200 ms and 7, 11, 21, 35, 42, 49, 63, 77, 84, 105, and 140 ms, respectively. The acquisition and equilibration times were 0.34 and 1.5 s, respectively, for the T_1 and $T_{1\rho}$ experiments, and 0.34 and 3.5 s for the heteronuclear NOE measurements. The complex time-domain data matrices for T_1 and NOE measurements were 128 × 2048 points; after zero-filling, Gaussian window multiplication, Fourier transform, and baseline correction, they gave spectra with digital resolutions of 1.5 and 35 Hz/pt in F2 and F1 dimensions, respectively. $T_{1\rho}$-weighted spectra were recorded for three different offset values (54, 72, and 102 ppm) in the F1 dimension, which coincided with the offset values for the spin-locking field. The spectral windows and data matrices consequently were reduced to give the digital resolutions of 1.5 and 23 Hz/pt in F2 and F1, respectively. For each T_1 and $T_{1\rho}$ experiment, 64 scans were accumulated per t_1 increment; for NOESY experiments 128 scans per t_1 value were acquired.

Following routine procedures, ^{31}P T_1 and $T_{1\rho}$ relaxation measurements were performed at 202.4 and 121.4 MHz (on Bruker AM-500 and AC-300 instruments, respectively) at 305 K.

Data evaluation

The intensities, $I(T)$, of cross-peaks in the T_1 and $T_{1\rho}$ experiments depicted in Fig. 1 are described with a single exponential decay (Sklenár et al., 1987)

$$I(T) = I_0 \exp\left(-\frac{T}{T_{1(\rho)}}\right), \tag{1}$$

where I_0 is the intensity at $T = 0$. The NOE enhancements η are

$$\eta = \frac{I_{sat}}{I_{unsat}} - 1, \tag{2}$$

where I_{sat} and I_{unsat} are the intensities of the cross-peaks in heteronuclear NOESY spectra obtained with and without saturation of the proton magnetization, respectively. The following relationships give a good approximation of the relaxation of the methine carbons by a single ^{13}C/^{1}H dipolar mechanism (Abragam, 1961):

$$\frac{1}{T_1} = \frac{D_{CH}^2}{10}[J(\omega_H - \omega_C) + 3J(\omega_C) + 6J(\omega_H + \omega_C)] \tag{3}$$

$$\frac{1}{T_{1\rho}} = \frac{D_{CH}^2 \sin^2\beta}{20}[4J(0) + J(\omega_H - \omega_C) + 3J(\omega_C) + 6J(\omega_H) + 6J(\omega_H + \omega_C)] \tag{4}$$

$$\eta = \frac{\gamma_H[6J(\omega_H + \omega_C) - J(\omega_H - \omega_C)]}{\gamma_C[J(\omega_H - \omega_C) + 3J(\omega_C) + 6J(\omega_H + \omega_C)]}, \tag{5}$$

where the dipolar coupling constant D_{CH} = 131.2 kHz (Kovacs et al., 1989), γ_H and γ_C are proton and carbon gyromagnetic ratios, and β is the tip angle of the effective field in the rotating frame (Peng et al., 1991). The angle $\beta = \arctan(\omega_1/\Delta\omega)$, where $\Delta\omega$ is the resonance offset and ω_1 is the effective spin-locking field strength (in most of our experiments $\omega_1/2\pi \approx 3.7$ kHz, so $\beta > 70°$). In writing Eq. 4 we assumed that all molecular rotational motions are much faster than ω_1. This is well justified because $T_{1\rho}$ values obtained at two different strengths of spin-locking fields (1.5 and 3.7 kHz) were found to be essentially the same. The spectral density functions, $J(\omega)$, featured in Eqs. 3–5 depend on both the overall motion of the aggregate and the internal motions of the ^{13}C-^{1}H bond vector. If the molecular dynamics are described by only two different correlation times, τ_m for the overall and τ_i for the internal motions, spectral densities are expressed in the form (Lipari and Szabo, 1982; Chachaty, 1987; Elbayed et al., 1989)

$$J(\omega) = S^2 \frac{\tau_m}{1 + \omega^2\tau_m^2} + (1 - S^2)\frac{\tau_e}{1 + \omega^2\tau_e^2}, \tag{6}$$

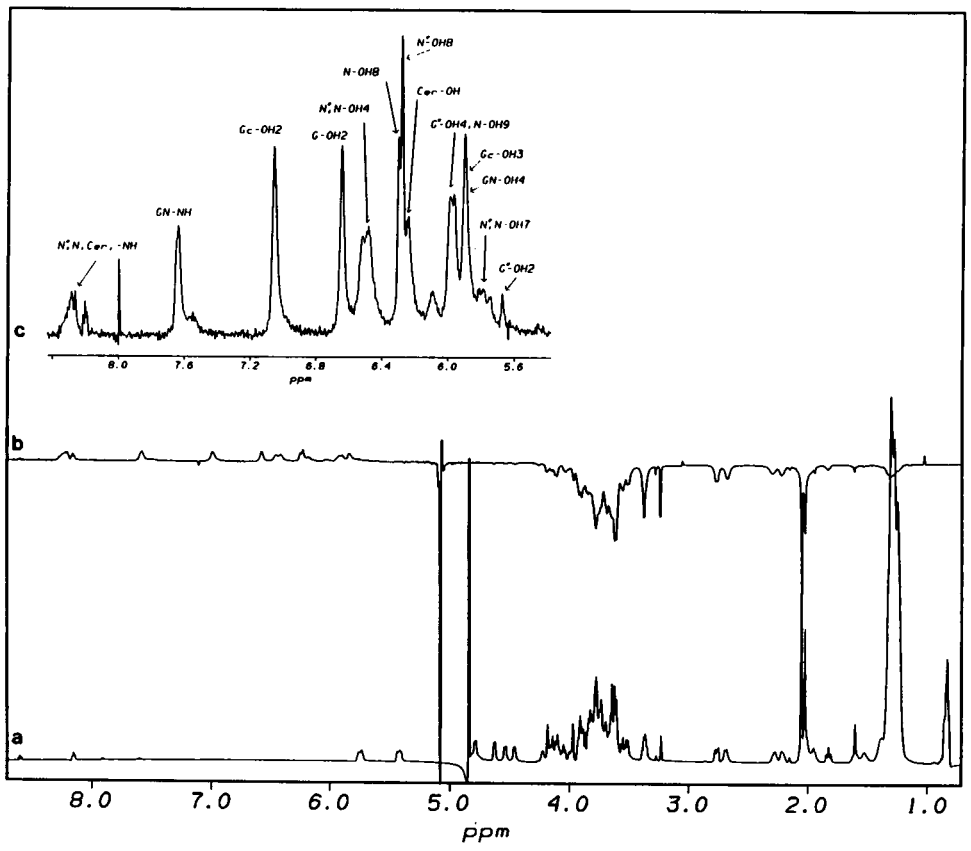

FIGURE 2 ^{1}H-NMR spectra of the GD1a/DPC micelles in aqueous solutions: (*a*) D_2O at 305 K; (*b*) 90%H_2O/10%D_2O at 273 K, obtained with the 1-$\bar{1}$ echo water suppression technique; (*c*) expansion of the hydroxyl proton region from (*b*). Throughout the figures, the GD1a glycosyl residues are indicated as follows: Gc for Glc, G for Gal, GN for GalNAc, G′ for Gal′, N for NeuAc and N′ for NeuAc′ (see also Scheme 1).

TABLE 1 Chemical shifts* of nonlabile (at 305 K) and labile (at 273 K) protons in GD1a/DPC micelles in H_2O solution

Proton	Cer	Glc	Gal	NeuAc	GalNAc	Gal′	NeuAc′
H1 *pro*S‡	4.18	4.48	4.55		4.82	4.64	
H1′ *pro*R	3.79						
H2	3.95	3.35	3.38		4.07	3.56	
OH2		6.95	6.60			5.62	
H3eq	4.10	3.65	3.62	2.72	3.83	4.11	2.78
H3ax				1.91			1.80
OH3	6.20	5.85					
H4	5.45*	3.63	4.15	3.82	4.19	3.97	3.72
OH4				6.45	5.85	5.95	6.41
H5	5.75	3.61	3.78	3.83	3.75	3.69	3.86
H6		3.82	3.83	3.53	3.79	3.75	3.65
H6′		4.00	3.83		3.79	3.75	
OH6		5.41	n.d.		n.d.	n.d.	
H7				3.61			3.61
OH7				5.75			5.75
H8				3.78			3.91
OH8				6.25			6.22
H9				3.66			3.67
H9′				3.89			3.90
OH9				3.66			n.d.
NH	8.22			8.25	7.60		8.25
CH_3				2.08	2.03		2.08

* Referenced to tetramethylsilane indirectly by setting δ Cer H4 to 5.45 ppm.
‡ The H1 signals for Cer were stereospecifically assigned on the basis of NOE and scalar coupling patterns.

where S^2 is an order parameter measuring the degree of spatial restriction of the internal motion and $\tau_e^{-1} = \tau_m^{-1} + \tau_i^{-1}$.

The T_1 and T_2 relaxation of ^{31}P in the deuterated phospholipid can be completely described by a chemical shift anisotropy mechanism (Abragam, 1961)

$$\frac{1}{T_1} = \frac{3}{10} C^2 \omega_P^2 J(\omega_P) \tag{7}$$

$$\frac{1}{T_2} = \frac{1}{20} C^2 \omega_P^2 [4J(0) + 3J(\omega_P)], \tag{8}$$

where C = 115.7 ppm, as obtained from the principal values of the ^{31}P chemical shift tensor (Dufourc et al., 1992). Utilizing inversion recovery and spin-locking techniques, the ^{31}P relaxation times were measured at 305 K for $\omega_P/2\pi$ = 202.4 and 121.4 MHz. Because the rotating frame relaxation time was measured on-resonance and showed no dependence on the effective field strength in the range of 0.5 to 3 kHz, it is equal to the transverse relaxation time.

RESULTS AND DISCUSSION

Headgroup conformation

The proton spectra of the GD1a/DPC system in aqueous solutions are shown in Fig. 2. Both spectra are clearly of high resolution, suggesting a molecular aggregate of relatively small size (vide infra). Spectral assignments of the ^1H (Table 1) and ^{13}C (Table 2) resonances were achieved through the performance of 1D TOCSY, 2D HSQC, and 2D HSQC-NOESY (recorded with and without carbon decoupling) experiments. The last experiment proved to be particularly useful in assigning spatially proximal H4, H5, H6, and H6′ spin systems in galactose residues. Tracing spin topology through scalar couplings was restricted in these cases by the small (<1 Hz) H4-H5 coupling constant. Similarly, the hydroxyl protons, due to their short T_2 times, were assigned on the basis of spatial proximity to the ring protons, rather than by scalar connectivities. These assignments were substantiated by 1D TOCSY experiments for the GD1a oligosaccharide dissolved in a mixed solvent, $H_2O/(CD_3)_2CO$ (4:1, v/v) at 263 K, where chemical exchange effects were eliminated (data not shown). It is worth noting that only the primary hydroxyl protons of the sialic acid and galactose residues were not observable (Table 1), probably due to the faster chemical exchange with the solvent protons. Another striking observation is that the OH8 protons (see Figs. 2 *c* and

TABLE 2 Carbon chemical shifts* of GD1a/DPC micelles in D_2O solution at 305 K

Carbon	Cer	Glc	Gal	NeuAc	GalNAc	Gal′	NeuAc′
C1	69.97	103.35	103.03	101.84	102.87	104.80	100.13
C2	53.56	73.00	70.30	174.30‡	51.33	69.48	174.28‡
C3	71.20	74.50	74.74	37.55	80.92	75.87	40.00
C4	130.46	79.27	77.44	68.97	68.10	67.82	68.75
C5	133.70	75.07	72.55	51.99	74.66	74.95	52.06
C6		60.50	60.97	73.38	61.45	61.27	73.15
C7				68.42			68.55
C8				74.50			72.14
C9				63.18			62.90
C=O	174.95‡			175.38‡	174.88‡		175.30‡

* Referenced to Gal′ C1 resonance at δ 104.8 ppm (compare Sabesan et al., 1991).
‡ Assigned on the basis of a semiselective HMBC experiment.

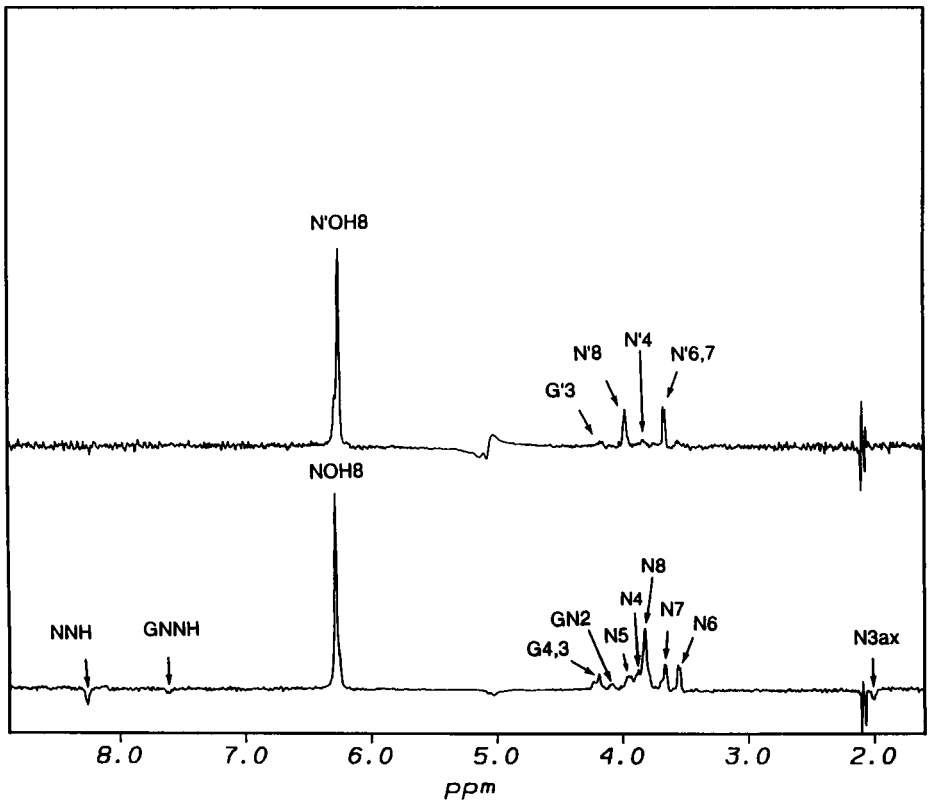

FIGURE 3 Truncated NOE spectra (0.35 s irradiation time) for the NeuAc (N) and NeuAc′ (N′) OH8 protons in GD1a at 281 K obtained using the 1-$\bar{1}$ echo water suppression technique. Note the nonuniform excitation profile. The residual water signal was reduced by post-acquisition data manipulation. In contrast to the upper trace, the lower trace spectrum shows significant spin-diffusion effects.

3) of both sialic acid residues share the same spectral features (slow chemical exchange, small vicinal coupling constant, and strong NOE contact to the ring H6 proton) reminiscent of a unique side-chain conformation in sialic-acid residues (Poppe and van Halbeek, 1991).

The interresidual $^1H/^1H$ NOE contacts observed for micellar GD1a are listed in Table 3. No attempts were made to quantitate the NOE interactions. Instead, all efforts were concentrated on proving their existence as direct NOE contacts. The data confirmed the arrangement of the GalNAc[NeuAc]-Gal trisaccharide fragment as being similar to that found in the previous study on the homologous GM1 ganglioside (Acquotti et al., 1990). In GD1a, the proximity of the GalNAc and NeuAc residues is proven by the NeuAc OH8/GalNAc NH and NeuAc OH8/GalNAc H2 NOE contacts (Fig. 3). The second contact is not direct, as inferred from the molecular model; it arises due to an interresidual interaction, for example, between NeuAc OH8/GalNAc NH or NeuAc OH8/GalNAc H3(H5), the latter of which could not be observed due to spectral overlap.

TABLE 3 Interresidual $^1H/^1H$ NOE contacts in GD1a/DPC micelles in aqueous solution

Residue ↓ /residue →	NeuAc′	Gal′	GalNAc	NeuAc	Gal	Glc	Cer
NeuAc′		OH8/H3 H3ax/H3					
Gal′	OH2/H3eq H3/H8		H1/H3 H1/H4 H1/H2				
GalNAc	CH_3/H8				CH_3/H2 H1/H4		
NeuAc			OH8/NH OH8/H2*		H3ax/H3 OH8/H4		
Gal				OH2/H3eq		H1/H4 H1/H6′ OH2/H6	
Glc					OH3/H1		H1/H1′ H1/H2 H1/H3 OH2/NH‡

* This NOE originates from spin diffusion effects.

‡ Could not be distinguished from the direct chemical exchange interaction.

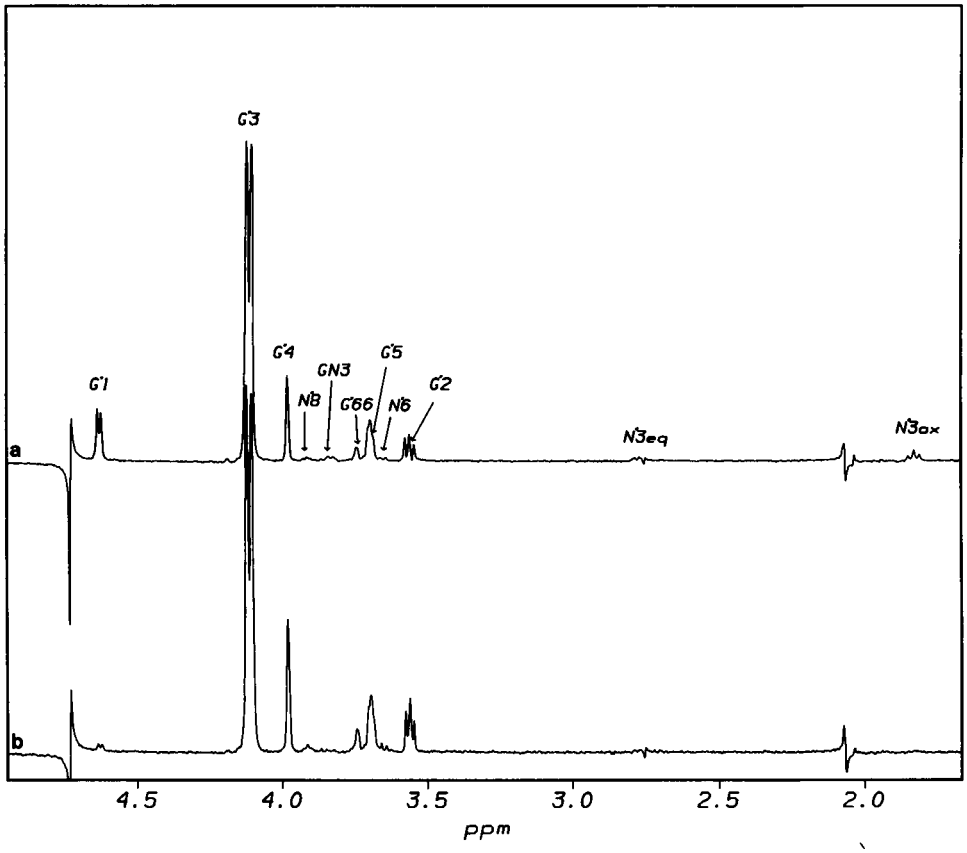

FIGURE 4 Double-selective TOCSY-NOESY spectra of GD1a/DPC in H_2O with selective irradiation of the Gal′ (G′) H1 and Gal′ H3 resonances. (*a*) Mixing times for the TOCSY and NOESY steps were 0.06 and 0.5 s, respectively. (*b*) The same as (*a*) but with double-DANTE saturation of Gal′ H1 and NeuAc′ H3ax resonances during the NOESY mixing time. Thus, spin diffusion effects (for example, Gal′ H3→Gal′ H1→ GalNAc H3 occurring in (*a*)) have been eliminated.

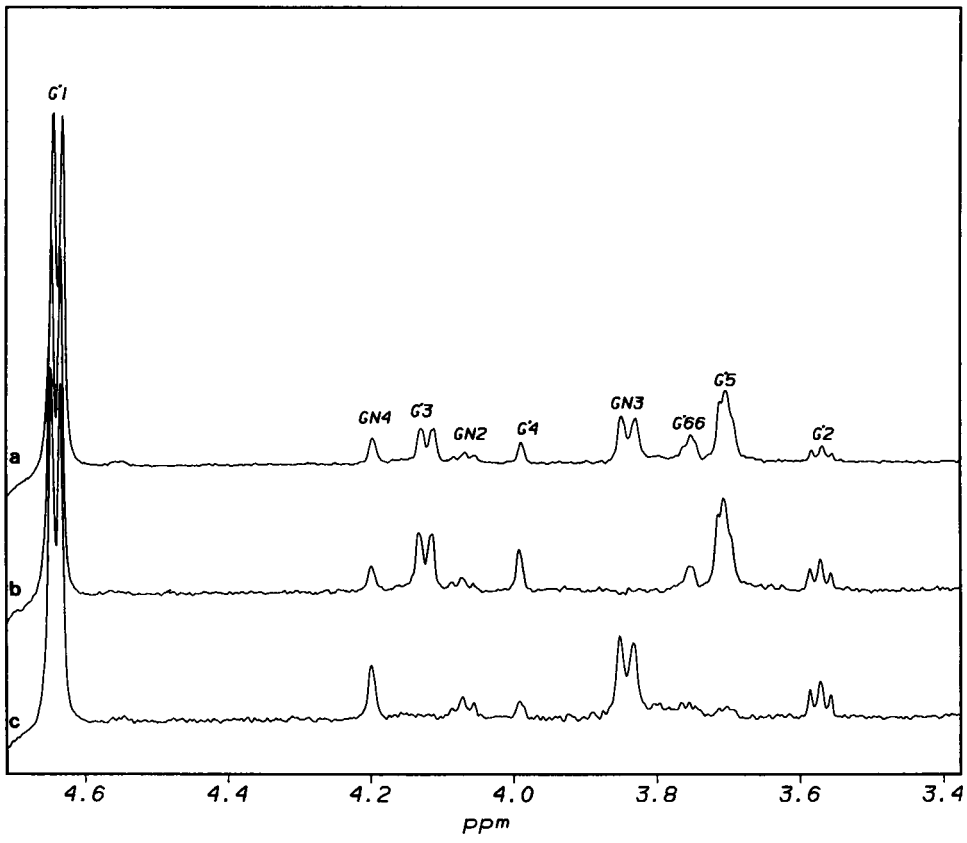

FIGURE 5 1D NOESY of GD1a/DPC in D_2O with selective excitation of Gal′ H1. (*a*) 0.5 s mixing time. (*b*) The same as in (*a*) but with irradiation of the GalNAc H3 spin during the mixing time. The indirect magnetization transfers mediated by the GalNAc H3 spin have been blocked. (*c*) The same as in (*a*) but with irradiation of the Gal′ H3 and Gal′ H5 spins with double-DANTE pulse train during the mixing time. In contrast to (*a*) the spectrum shows only the direct contribution to the Gal′ H1/Gal′ H4 magnetization transfer peak.

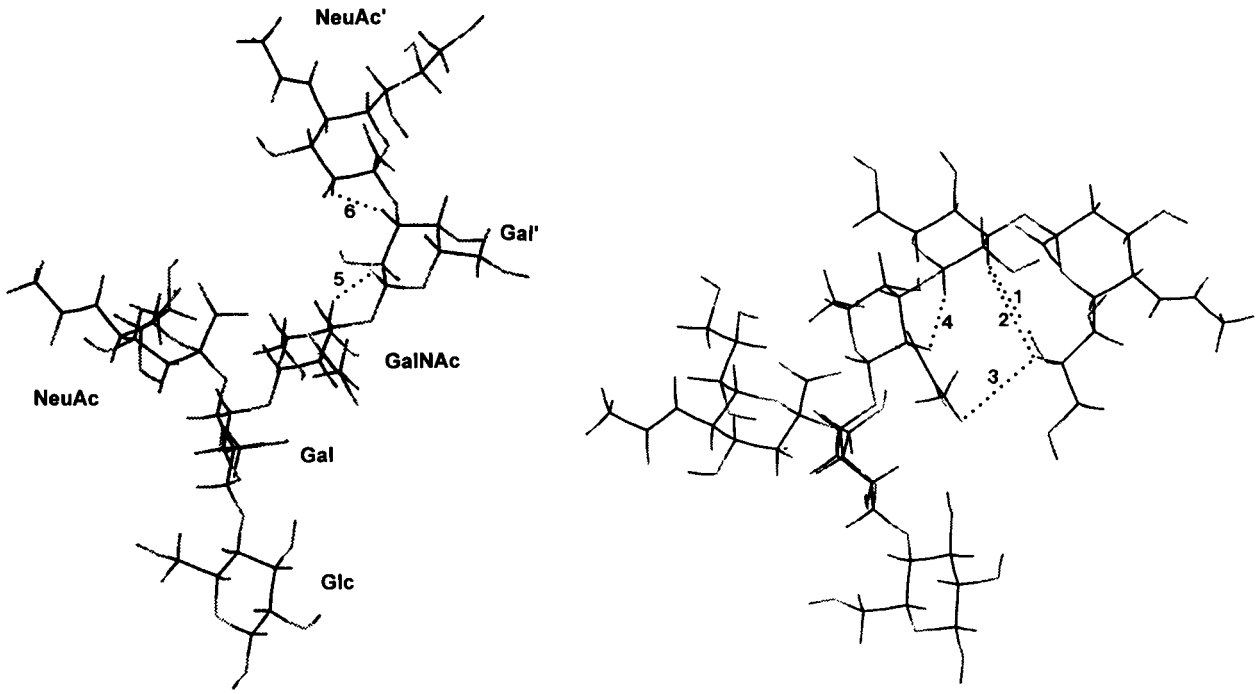

FIGURE 6 Molecular models of the GD1a headgroup. This picture serves to illustrate, in a qualitative fashion, two energetically allowed structures that satisfy the mutually exclusive sets of NOE constraints {**1**, **2**, **3**, **4**} and {**5**, **6**}, respectively. These NOE contacts (dotted lines) correspond to: 1: NeuAc′ OH8/Gal′ H3; 2: NeuAc′ H8/Gal′ H3; 3: NeuAc′ H8/GalNAc CH_3; 4: Gal′ H1/GalNAc H2; 5: Gal′ H1/GalNAc H4; 6: NeuAc′ H3ax/Gal′ H3.

An interesting NOE pattern was found for the NeuAc′-Gal′GalNAc fragment revealing multiple conformations for both glycosidic linkages. For example, the NeuAc′ H3ax/Gal′ H3 and NeuAc′ OH8/Gal′ H3 NOE contacts, measured in 1D double-selective TOCSY-NOESY and TOCSY-MINSY experiments (see Fig. 4), can only occur simultaneously if the NeuAc′α2→3Gal′ glycosidic linkage samples both (180°, 0°) and (−60°, 0°) conformations. In contrast, the NOE pattern for the same type of linkage, NeuAcα2→3Gal, is completely different, showing an NeuAc H3ax/Gal H3 interaction that is 6 times stronger than for NeuAc′ H3ax/Gal′ H3, and the additional NeuAc OH8/Gal H4 contact, which strongly suggests the existence of only the (180°, 0°) conformation. Conformational averaging is also evident for the Galβ1→3GalNAc linkage, where Gal′ H1/GalNAc H2 and Gal′ H1/GalNAc H4 contacts (Fig. 5) are unlikely to occur for only one set of glycosidic angles. Based on the distance mapping procedure outlined by Acquotti et al. (1990), this linkage may sample several conformations with (Φ, Ψ) values around (40°, 30°), (40°, −30°) and (−30°, −30°). More compelling evidence for conformational averaging comes from a long-range GalNAc CH_3/NeuAc′ H8 NOE. As inferred from a molecular model, this contact can occur only in conformations in which the NeuAc′ H3ax/Gal′ H3 and Gal′ H1/GalNAc H4 separations are too large to yield a detectable NOE interaction. Fig. 6, presenting two energetically allowed conformations of the GD1a headgroup, may serve to visualize better the extent of conformational variation. The dotted lines indicate the NOE contacts that are exclusive for each conformation.

Finally, a few interactions were observed between the glucose and ceramide protons, giving some insight into the orientation of the headgroup at the membrane surface. Here, the most important observation is direct magnetization transfer between Cer NH and Glc OH2 protons by NOE and/or chemical exchange mechanisms. The proximity of these protons is consistent with the structure found by x-ray (Nyholm et al., 1990) and molecular mechanics studies (Nyholm and Pascher, 1993) in which the glucose unit occupies layer-parallel orientation. This corresponds to the ganglioside adopting, for a significant amount of time, an L-shaped conformation in which the headgroup is bent toward the micellar surface. With the presented data, however, it is not possible to determine if the headgroup orientation is unique or if it adopts multiple conformations (Nyholm and Pascher, 1993), both layer-parallel and layer-perpendicular.

More insight into the conformational averaging within the oligosaccharide portion of GD1a was gained from the ^{13}C relaxation studies presented in the next section.

Headgroup dynamics

The overall motion of the micellar aggregate was probed first by ^{31}P relaxation measurements at two different field strengths corresponding to ^{31}P resonance frequencies of 121.4 and 202.4 MHz. Because the dodecylphosphocholine is fully deuterated, the ^{31}P relaxes almost exclusively by a chemical shift anisotropy mechanism given by Eqs. 7 and 8. The relaxation rates were used to calculate the motional parameters of the two-state model given by Eq. 6 (see Table 4).

TABLE 4 Measured* and calculated‡ ^{31}P relaxation times of GD1a/DPC micelles at 305 K

Field [MHz]	T_1^{exp} [s]	T_1^{calc} [s]	T_2^{exp} [s]	T_2^{calc} [s]
202.4	1.34	1.36	0.22	0.19
121.4	2.76	2.82	0.38	0.51

* Standard errors did not exceed 5% of the experimental values.
‡ Calculated using Eqs. 6–8 with $\tau_m = 5.07$ ns, $\tau_i = 0.12$ ns, and $S^2 = 0.21$ obtained from a nonlinear least-squares optimization.

The correlation time for the overall tumbling, $\tau_m = 5.07$ ns, corresponds to a molecular weight of 12–16 kDa, consistent with previous physicochemical studies of DPC micelles (Lauterwein et al., 1979). Thus, we may conclude that micelles that contain one GD1a molecule per 30 ± 10 phospholipid molecules are statistically the most probable.

Using proton detection as described in Materials and Methods, the GD1a headgroup dynamics were probed by ^{13}C

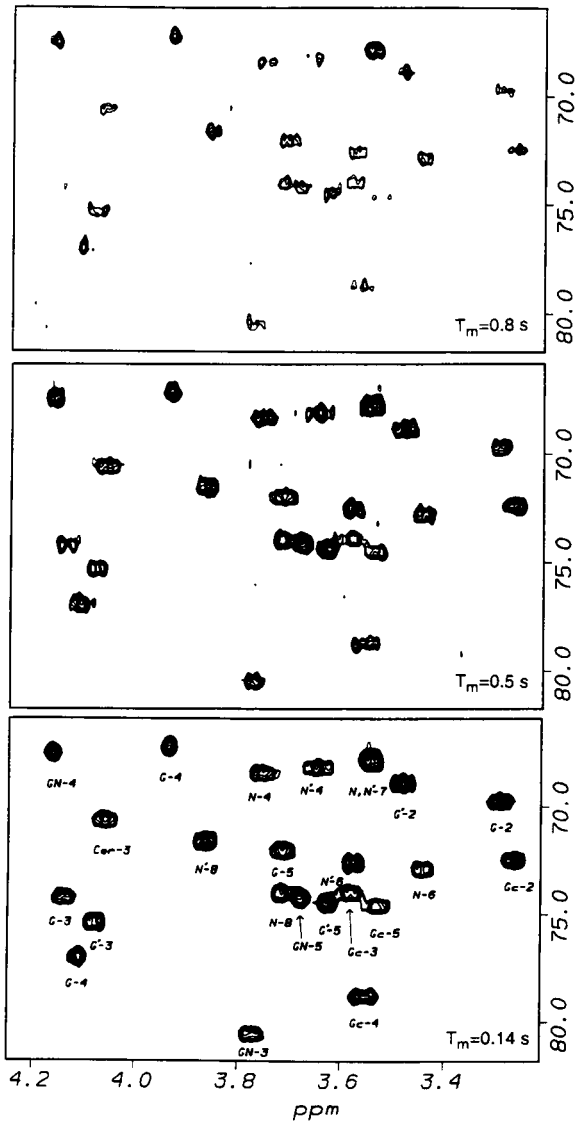

FIGURE 7 Expansions of the 2D ^1H-detected, T_1-weighted, ^{13}C-^1H correlation spectra of GD1a/DPC micelles in D_2O at the indicated mixing times.

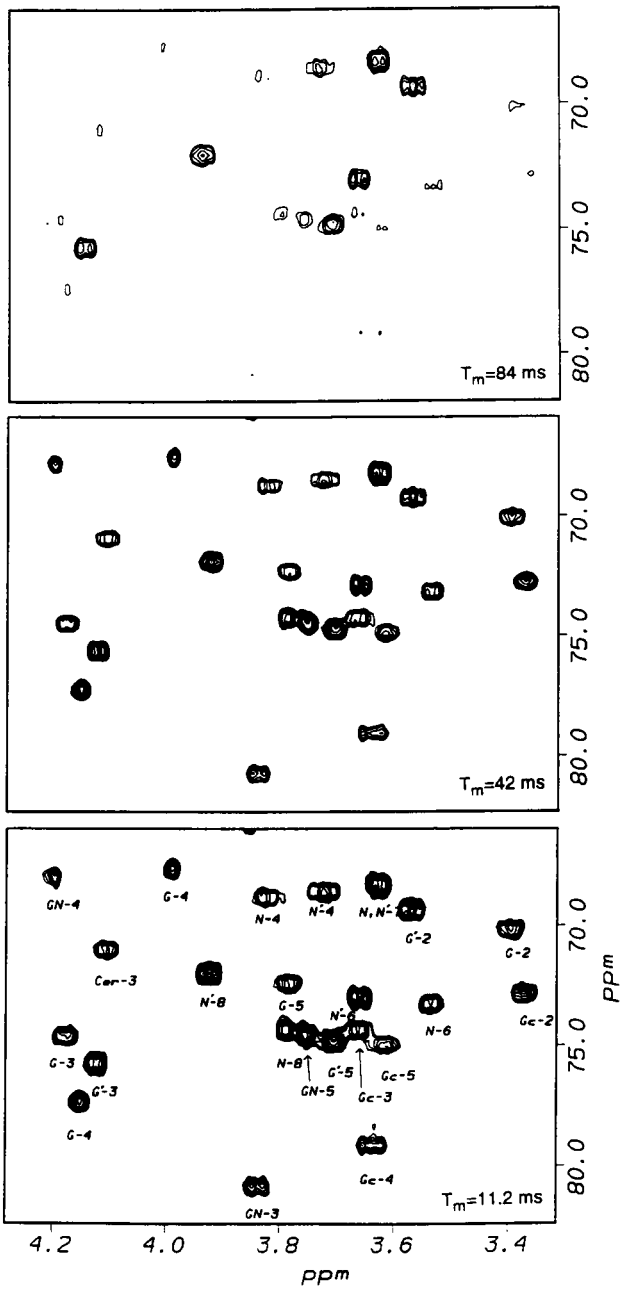

FIGURE 8 Expansions of the 2D ^1H-detected, $T_{1\rho}$-weighted, ^{13}C-^1H correlation spectra of GD1a/DPC micelles in D_2O at the indicated mixing times.

T_1, $T_{1\rho}$, and NOE measurements. Examples of 2D spectra are presented in Figs. 7 and 8. With the exception of the Gal′ C4 spin (vide infra), the data in Table 5 clearly show significantly different $T_{1\rho}$ and NOE values for the NeuAc′ and Gal′ residues as compared to the rest of the carbohydrate moiety. The relaxation data were converted into motional parameters using Eqs. 1–6, assuming a single correlation time for the GalNAc[NeuAc]GalGlc fragment and two correlation times for the NeuAc′Gal′ branch (Table 6). The presence of the fast internal motions of the NeuAc′ and Gal′ residues, reflected in the τ_i and S^2 parameters, agrees with the discussed conformational averaging of the NeuAc′α2→3Gal′ and

TABLE 5 Relaxation parameters (nT_1 [s], $nT_{1\rho}$ [s], NOE)* for ^{13}C nuclei‡ in GD1a/DPC micelles in D_2O solution at 305 K

Residue	Parameter	C1	C2	C3	C4	C5	C6¶	C8	C9¶
NeuAc'	T_1			0.46	0.44	0.43	0.43	0.42	0.46
	$T_{1\rho}$			0.14	0.13	0.14	0.13	0.15	0.17
	NOE			1.6	1.6	1.6	1.6	1.7	1.6
Gal'	T_1	0.43	0.43	0.41	0.48	0.43	0.5		
	$T_{1\rho}$	0.14	0.15	0.15	0.07	0.14	0.22		
	NOE	1.5	1.7	1.6	1.2	1.5	2.05		
GalNAc	T_1	0.45	0.48	0.47	0.52	0.43	0.44		
	$T_{1\rho}$	0.07	0.08	0.07	0.06	0.08	0.16		
	NOE	1.1	1.2	1.1	1.2	1.2	1.9		
NeuAc	T_1			0.40	0.43	0.42	0.44	0.46	0.48
	$T_{1\rho}$			n.d.	0.08	0.08	0.08	0.08	0.13
	NOE			1.1	1.1	1.2	1.3	1.1	1.5
Gal	T_1	0.46	0.42	0.40	0.45	0.45	0.41		
	$T_{1\rho}$	0.07	0.08	0.08	0.08	0.07	0.16		
	NOE	1.1	1.1	1.0	1.0	1.1	1.7		
Glc	T_1	0.47	0.47	0.47	0.44	0.43	0.45		
	$T_{1\rho}$	0.08	0.08	0.08	0.08	0.08	0.09		
	NOE	1.2	1.2	1.2	1.3	1.2	1.4		
Cer	T_1		0.45	0.47					
	$T_{1\rho}$		0.07	0.08					
	NOE		1.2	1.4					

* The estimated average standard error is 10% for T_1 and $T_{1\rho}$ and 20% for NOE values.
‡ Data for the C7 atoms of NeuAc and NeuAc' residues are not included in the analysis because of spectral overlap.
¶ The relaxation parameters for the methylene carbons should be treated with caution since they might contain systematic errors due to cross-correlation effects (Werbelow and Grant, 1977; Kay and Bull, 1992).

Gal'β1→3GalNAc linkages. The different relaxation of the Gal' C4 nucleus might be explained by the fact that the torsions about the Gal' C1-O1 bond (Φ torsions) do not influence dipolar relaxation due to the parallel arrangement of the C4-H4 and C1-O1 bonds in galactose residues. The motional parameters listed in Table 6 should be interpreted with caution because they might not correspond to any physical motion. For example, the overall correlation time (~2.8 ns) is rather short for the expected size of the molecular aggregate (~12–16 kDa). This discrepancy, which arises from our oversimplified spectral density model, suggests that, in addition to the micellar tumbling, another segmental and/or overall motion of the GD1a headgroup uniformly contribute to the dipolar relaxation of the carbon spins. However, a more rigorous treatment of the molecular motions of the system is not warranted by our data.

The ^{13}C T_1 values obtained for GD1a in this study (Table 5), and independently by Sabesan et al. (1991) for the GD1aOS oligosaccharide, are roughly uniform across all sugar units, deceptively suggesting that the motion of the headgroup is isotropic. Unlike the micellar GD1a, however, the overall motion of the GD1aOS molecule occurs on a similar time scale as the internal motion, masking the contribution of the latter to the spectral densities.

CONCLUSIONS

By means of multinuclear magnetic resonance spectroscopy, we have investigated the conformation and conformational dynamics of the GD1a ganglioside anchored into a micelle. The choice of the micellar systems for these studies has certain important advantages (compare McDonnell and Opella, 1993). First, the micelle system mimics the membrane environment. The water molecules are less mobile in the vicinity of the micellar surface, and this slows down chemical exchange with the hydroxyl protons of the carbohydrate headgroup. At temperatures close to the freezing point of H_2O, most of the hydroxyl protons were observable, contributing valuable information to the conformational analysis. Finally, anchoring of the glycolipid in the micelle allowed the observation of intramolecular motions within the carbohydrate headgroup.

Contrary to the common perception of the GD1a carbohydrate adopting a single conformation, our NMR data clearly revealed the pronounced flexibility of the NeuAc'α2→3Gal' and Gal'β1→3GalNAc glycosidic linkages. It is not, however, straightforward to extrapolate this result to a real membrane. Our model consisted of a single ganglioside molecule per micelle, although

TABLE 6 Average ^{13}C relaxation rates and dynamics parameters* for GD1a/DPC micelles in aqueous solution

Residue	R_1 [s^{-1}]	R_2 [s^{-1}]	NOE	τ_m [ns]	τ_i [ns]	S^2
GalNAc, NeuAc, Gal, Glc	2.2 ± 0.2	12.5 ± 2.0	1.2 ± 0.2	2.8 ± 0.1	0	1
NeuAc', Gal'‡	2.3 ± 0.2	7.1 ± 1.0	1.6 ± 0.2	2.8 ± 0.1	0.34 ± 0.1	0.55 ± 0.08

* Obtained by nonlinear least-squares optimization using Eqs. 3–6. The relaxation data for the methylene carbons were not included in the analysis.
‡ With the exception of Gal' C4.

light-scattering experiments have shown that gangliosides aggregate within a membrane (Corti, 1985; Cantu' et al., 1990). Thus, the flexibility of the carbohydrate headgroup may be restricted in the natural environment (compare Jarrell et al., 1986; Winsborrow et al., 1992). Nevertheless, it is likely to play a crucial role in the membrane organization of the ganglioside molecules.

We thank Dr. John S. Harwood for access to the Bruker AC-300 spectrometer and Dr. Tim Thurlby for carefully reading the manuscript. This research is supported by National Institutes of Health grant P41-RR-05351 from the National Center for Research Resources.

REFERENCES

Abragam, A. 1961. Principles of Nuclear Magnetism. Clarendon Press, Oxford, UK. 599 pp.

Acquotti, D., L. Poppe, J. Dabrowski, C. W. von der Lieth, S. Sonnino, and G. Tettamanti. 1990. Three-dimensional structure of the oligosaccharide chain of GM1 ganglioside revealed by a distance-mapping procedure: a rotating and laboratory frame nuclear Overhauser enhancement investigation of native glycolipid in dimethyl sulfoxide and in water-dodecylphosphocholine solutions. *J. Am. Chem. Soc.* 112:7772–7778.

Aubin, Y., and J. H. Prestegard. 1993. Structure and dynamics of sialic acid at the surface of a magnetically oriented membrane system. *Biochemistry.* 32:3422–3428.

Bothner-By, A. A., R. L. Stephens, J.-M. Lee, C. D. Warren, and R. W. Jeanloz. 1984. Structure determination of a tetrasaccharide: transient nuclear Overhauser effects in the rotating frame. *J. Am. Chem. Soc.* 106: 811–813.

Boudot, D., C. Roumestand, F. Toma, and D. Canet. 1990. Pseudo-3D NMR of proteins with selective excitation by DANTE-Z. One-dimensional TOCSY-NOESY experiment. *J. Magn. Reson.* 90:221–227.

Cantu', L., M. Corti, S. Sonnino, and G. Tettamanti. 1990. Evidence for spontaneous aggregation phenomena in mixed micelles of gangliosides. *Chem. Phys. Lipids.* 55:223–229.

Chachaty, C. 1987. Applications of NMR methods to the physical chemistry of micellar solutions. *Prog. NMR Spectrosc.* 19:183–222.

Corti, M. 1985. Aggregation behaviour of gangliosides. *In* Physics of Amphiphiles: Micelles, Vesicles and Microemulsions. V. Degiorgio and M. Corti, editors. North-Holland, Amsterdam. 637–647.

Czarniecki, M. F., and E. R. Thornton. 1977. Carbon-13 nuclear magnetic resonance spin-lattice relaxation in the *N*-acylneuraminic acids. Probes for internal dynamics and conformational analysis. *J. Am. Chem. Soc.* 99:8273–8279.

Dufourc, E. J., C. Mayer, J. Stohrer, G. Althoff, and G. Kothe. 1992. Dynamics of phosphate head groups in biomembranes: comprehensive analysis using phosphorus-31 nuclear magnetic resonance lineshape and relaxation time measurements. *Biophys. J.* 61:42–57.

Eaton, H. L., and S. I. Hakomori. 1988. Conformation of micelle-bound gangliosides by 2D proton NMR spectroscopy. 195th ACS Natl. Mtg. 91-CARB. (Abstr.)

Elbayed, K., D. Canet, and J. Brondeau. 1989. Accurate determination of frequency dependent cross-relaxation terms in homonuclear and heteronuclear two spin-½ systems. Applications to dynamical studies of aromatic moieties in micellized surfactants. *Mol. Phys.* 68:295–314.

Fenske, D. B., K. Hamilton, H. C. Jarrell, E. Florio, K. R. Barber, and C. W. M. Grant. 1991. Glycosphingolipids: ^{2}H NMR study of the influence of carbohydrate headgroup structure on ceramide acyl chain behavior in glycolipid-phospholipid bilayers. *Biochemistry.* 30:4503–4509.

Fishman, P. H., and R. O. Brady. 1976. Biosynthesis and function of gangliosides. *Science.* 194:906–915.

Hakomori, S. I. 1984. Glycosphingolipids as markers for development and differentiation and as regulators of cell proliferation. *In* The Cell Membrane. E. Haber, editor. Plenum Press, New York. 181–201.

Hakomori, S. I. 1993. Structure and function of sphingoglycolipids in transmembrane signalling and cell-cell interactions. *Biochem. Soc. Trans.* 21: 583–595.

Jarrell, H. C., J. B. Giziewicz, and I. C. P. Smith. 1986. Structure and dynamics of a glyceroglycolipid: a ^{2}H NMR study of head group orientation, ordering, and effect on lipid aggregate *Biochemistry.* 25: 3950–3957.

Kay, L. E., T. L. Jue, B. Bangerter, and P. C. Demou. 1987. Sensitivity enhancement of ^{13}C T_1 measurements via polarization transfer. *J. Magn. Reson.* 73:558–564.

Kay, L. E., D. A. Torchia, and A. Bax. 1989. Backbone dynamics of proteins as studied by ^{15}N inverse detected heteronuclear NMR spectroscopy: application to *Staphylococcus nuclease. Biochemistry.* 28:8972–8979.

Kay, L. E., L. K. Nicholson, F. Delaglio, A. Bax, and D. A. Torchia. 1992. Pulse sequences for removal of the effects of cross correlation between dipolar and chemical-shift anisotropy relaxation mechanisms on the measurement of heteronuclear T_1 and T_2 values in proteins. *J. Magn. Reson.* 97:359–375.

Kay, L. E., and T. E. Bull. 1992. Heteronuclear transverse relaxation in AMX, AX_2, and AX_3 spin systems. *J. Magn. Reson.* 99:615–622.

Kovacs, H., S. Bagley, and J. Kowalewski. 1989. Motional properties of two disaccharides in solutions as studied by carbon-13 relaxation and NOE outside the extreme narrowing region. *J. Magn. Reson.* 85:530–541.

Lauterwein, J., C. Bösch, L. R. Brown, and K. Wüthrich. 1979. Physicochemical studies of the protein-lipid interactions in melittin-containing micelles. *Biochim. Biophys. Acta.* 556:244–264.

Lipari, G., and A. Szabo. 1982. Model-free approach to the interpretation of nuclear magnetic resonance relaxation in macromolecules. 1. Theory and range of validity. *J. Am. Chem. Soc.* 104:4546–4559.

London, R. E., and J. Avitabile. 1976. ^{13}C-{^{1}H} nuclear Overhauser enhancement and ^{13}C spin lattice relaxation in molecules undergoing multiple internal rotations. *J. Chem. Phys.* 65:2443–2451.

Marion, D., and K. Wüthrich. 1983. Application of phase-sensitive two-dimensional correlated spectroscopy (COSY) for measurements of ^{1}H-^{1}H spin-spin coupling constants in proteins. *Biochem. Biophys. Res. Commun.* 113:967–974.

Massefski, W., Jr., and A. G. Redfield. 1988. Elimination of multiple-step spin diffusion effects in two-dimensional NOE spectroscopy of nucleic acids. *J. Magn. Reson.* 78:150–155.

McDonnell, P. A., and S. J. Opella. 1993. Effect of detergent concentration on multidimensional solution NMR spectra of membrane proteins in micelles. *J. Magn. Reson. Series B.* 102:120–125.

Morris, G. A., and R. Freeman. 1978. Selective excitation in Fourier transform nuclear magnetic resonance. *J. Magn. Reson.* 29:433–462.

Neuhaus, D., and M. P. Williamson. 1989. The nuclear Overhauser effect in structural and conformational analysis. VCH, New York. 522 pp.

Nirmala, N. R., and G. Wagner. 1989. Measurement of ^{13}C spin-spin relaxation times by two-dimensional heteronuclear ^{1}H-^{13}C correlation spectroscopy. *J. Magn. Reson.* 82:659–661.

Nyholm, P.-G., I. Pascher, and S. Sundell. 1990. The effect of hydrogen bonds on the conformation of glycosphingolipids. Methylated and unmethylated cerebroside studied by X-ray single crystal analysis and model calculation. *Chem. Phys. Lipids.* 52:1–10.

Nyholm, P.-G., and I. Pascher. 1993. Orientation of the saccharide chains of glycolipids at the membrane surface: conformational analysis of the glucose-ceramide and the glucose-glyceride linkages using molecular mechanics (MM3). *Biochemistry.* 32:1225–1234.

Palmer, A. G., III, M. Rance, and P. E. Wright. 1991. Intramolecular motions of a zinc finger DNA-binding domain from Xfin characterized by proton-detected natural abundance ^{13}C heteronuclear NMR spectroscopy. *J. Am. Chem. Soc.* 113:4371–4380.

Peng, J. W., V. Thanabal, and G. Wagner. 1991. 2D heteronuclear NMR measurements of spin-lattice relaxation times in the rotating frame of X nuclei in heteronuclear HX spin systems. *J. Magn. Reson.* 94:82–100.

Peng, J. W., and G. Wagner. 1992. Mapping of spectral density functions using heteronuclear NMR relaxation measurements. *J. Magn. Reson.* 98: 308–332.

Poppe, L., C. W. von der Lieth, and J. Dabrowski. 1990. Conformation of the glycolipid globoside head group in various solvents and in the micelle-bound state. *J. Am. Chem. Soc.* 112:7762–7771.

Poppe, L., and H. van Halbeek. 1991. Nuclear magnetic resonance of hydroxyl and amido protons of oligosaccharides in aqueous solution: evidence for a strong intramolecular hydrogen bond in sialic acid residues. *J. Am. Chem. Soc.* 113:363–365.

Poppe, L., and H. van Halbeek. 1992. NOE measurements on carbohydrates in aqueous solution by double-selective pseudo-3D TOCSY-ROESY and TOCSY-NOESY. Application to gentiobiose. *J. Magn. Reson.* 96: 185–190.

Sabesan, S., K. Bock, and R. U. Lemieux. 1984. The conformational properties of the gangliosides GM2 and GM1 based on ^{1}H and ^{13}C nuclear magnetic resonance studies. *Can. J. Chem.* 62:1034–1045.

Sabesan, S., J. Ø. Duus, T. Fukunaga, K. Bock, and S. Ludvigsen. 1991. NMR and conformational analysis of ganglioside GD1a. *J. Am. Chem. Soc.* 113:3236–3246.

Sanders, C. R., II, and J. H. Prestegard. 1991. Orientation and dynamics of β-dodecyl glucopyranoside in phospholipid bilayers by oriented sample NMR and order matrix analysis. *J. Am. Chem. Soc.* 113:1987–1996.

Scarsdale, J. N., R. K. Yu, and J. H. Prestegard. 1986. Structural analysis of a glycolipid head group with one- and two-state NMR pseudoenergy approaches. *J. Am. Chem. Soc.* 108:6778–6784.

Scarsdale, J. N., J. H. Prestegard, and R. K. Yu. 1990. NMR and computational studies of interactions between remote residues in gangliosides. *Biochemistry.* 29:9843–9855.

Skarjune, R., and E. Oldfield. 1979. Physical studies of cell surface and cell membrane structure. *Biochim. Biophys. Acta.* 556:208–218.

Sklenár, V., D. Torchia, and A. Bax. 1987. Measurement of carbon-13 longitudinal relaxation using ^{1}H detection. *J. Magn. Reson.* 73:375–379.

Sklenár, V., and A. Bax. 1987. Spin-echo water suppression for the generation of pure-phase two-dimensional NMR spectra. *J. Magn. Reson.* 74:469–479.

Sklenár, V., and J. Feigon. 1990. Simplification of DNA proton nuclear magnetic resonance spectra by homonuclear Hartmann-Hahn edited two-dimensional nuclear Overhauser enhancement spectroscopy. *J. Am. Chem. Soc.* 112:5644–5645.

Subramanian, S., and A. Bax. 1987. Generation of pure phase NMR subspectra for measurement of homonuclear coupling constants. *J. Magn. Reson.* 71:325–330.

Tettamanti, G., F. Bonali, S. Marchesini, and V. Zambotti. 1973. A new procedure for the extraction, purification and fractionation of brain gangliosides. *Biochim. Biophys. Acta.* 296:160–170.

Werbelow, L. G., and D. M. Grant. 1977. Intramolecular dipolar relaxation in multispin systems. *Adv. Magn. Reson.* 9:189–299.

Winsborrow, B. G., I. C. P. Smith, and H. C. Jarrell. 1991. Dynamics of glycolipids in the liquid-crystalline state. ^{2}H NMR study. *Biophys. J.* 59:729–741.

Winsborrow, B. G., J.-R. Brisson, I. C. P. Smith, and H. C. Jarrell. 1992. Influence of the membrane surface on glycolipid conformation and dynamics: an interpretation of NMR results using conformational energy calculations. *Biophys. J.* 63:428–437.